ENVIRONMENTAL RESEARCH
LETTERS

LETTER

OPEN ACCESS

RECEIVED
14 May 2023

REVISED
11 July 2023

ACCEPTED FOR PUBLICATION
18 July 2023

PUBLISHED
17 August 2023

Is a wet-bulb temperature of 35 °C the correct threshold for human survivability?

Yi-Chuan Lu[1,2,*] and **David M Romps**[2,3]

[1] Department of Physics, University of California, Berkeley, Berkeley, CA, United States of America
[2] Climate and Ecosystem Sciences Division, Lawrence Berkeley National Laboratory, Berkeley, CA, United States of America
[3] Department of Earth and Planetary Science, University of California, Berkeley, Berkeley, CA, United States of America
[*] Author to whom any correspondence should be addressed.

E-mail: yclu@berkeley.edu

Keywords: heat index, wet-bulb temperature, survivability

Abstract

A wet-bulb temperature of 35 °C is widely used as the threshold for human survivability, but the wet-bulb temperature is not a particularly accurate metric for human heat stress. For a person in the shade, a more accurate metric is the heat index, which is based on a model of human thermoregulation that accounts for metabolic heat, radiation, respiratory ventilation, and finite wind speeds. The heat index has two critical values: the highest heat index for which a healthy core temperature can be maintained and the highest heat index that is survivable. It is shown here that a wet-bulb temperature of 35 °C corresponds to conditions between these two critical values. For example, in a world warmer than pre-industrial by 10 °C, about 30% of the world's population would be exposed once or more per year to a wet-bulb temperature above 35 °C, but the heat index reveals that less than 2% would be exposed to fatal conditions while over 60% would be exposed to conditions that would cause hyperthermia.

1. Introduction

A wet-bulb temperature of 308 K (35 °C, 95 °F) is widely used as the threshold for human survivability in the field of climate science (Sherwood and Huber 2010, Pal and Eltahir 2016, Schär 2016, Coffel *et al* 2017, Im *et al* 2017, 2018, Sherwood 2018, Monteiro and Caballero 2019, Raymond *et al* 2020, Ramsay *et al* 2021, Rogers *et al* 2021, Saeed *et al* 2021). Despite its use as a predictor of human heat stress, the wet-bulb temperature is defined as the equilibrium temperature of a wetted thermometer in high winds. Since the Lewis number of air is near one, the energy balance of a wetted thermometer can be approximated mathematically as

$$\sigma\left(T^4 - T_{\mathrm{rad}}^4\right) + f(u)\left\{c_{\mathrm{p}}\left(T - T_{\mathrm{a}}\right) + L\left[q_v^*\left(T\right) - q_{\mathrm{a}}\right]\right\} = 0\,, \tag{1}$$

where T is the temperature of the wetted thermometer, T_{a} is the air temperature, q_a is the specific humidity, ρ is the air density, c_{p} is the heat capacity of air at constant pressure, T_{rad} is the effective radiating temperature of the surrounding surfaces, L is the latent heat of vaporization of water, q_v^* is the saturated specific humidity, u is the wind speed, and $f(u)$ is an effective mass flux of turbulent exchange between air and the thermometer. When u is large, $f(u)$ is large and the turbulent enthalpy fluxes (sensible plus latent) dominate the energy balance. In that special case, we refer to the temperature T of the wetted thermometer as the wet-bulb temperature T_{w}, which is defined by

$$c_{\mathrm{p}}\left(T_{\mathrm{w}} - T_{\mathrm{a}}\right) + L\left[q_v^*\left(T_{\mathrm{w}}\right) - q_{\mathrm{a}}\right] = 0\,. \tag{2}$$

The reason T_{w} is potentially relevant to human heat stress is because we can write the enthalpy fluxes off of a human's sweat-covered skin in terms of T_{w}. For any u, if the sweaty skin has a temperature T_{s}, the turbulent enthalpy flux from skin to the air is

$$F = f(u)\left\{c_{\mathrm{p}}\left(T_{\mathrm{s}} - T_{\mathrm{a}}\right) + L\left[q_v^*\left(T_{\mathrm{s}}\right) - q_{\mathrm{a}}\right]\right\} \tag{3}$$

$$= f(u)\left\{c_{\mathrm{p}}\left(T_{\mathrm{s}} - T_{\mathrm{w}}\right) + L\left[q_v^*\left(T_{\mathrm{s}}\right) - q_v^*\left(T_{\mathrm{w}}\right)\right]\right\}, \tag{4}$$

where equation (2) has been used in the second line to eliminate T_{a} and q_{a} in favor of T_{w}. In other words, the air feels the same as saturated air at temperature T_{w}. Equation (4) implies that whenever the wet-bulb temperature T_{w} is greater than the skin temperature

T_s, the net flow of sensible and latent heat is into the skin.

For this reason, Sherwood and Huber (Sherwood and Huber 2010, SH10 hereafter) argued that exposure to $T_w \gtrsim 308$ K (35 °C, 95 °F) for more than a few hours would be fatal. As the argument goes, with a standard core temperature $T_c = 310$ K (37 °C, 98.6 °F) and a basal metabolic rate of 50 W per square meter of skin area (hereafter written as 50 W m^{-2}), the body will move heat from the core to the skin at that rate by keeping the skin temperature T_s at 308 K or below. If $T_w \gtrsim 308$ K, the skin temperature must be greater than 308 K to release heat to the air, but then the body cannot move metabolic heat from the core to the skin at the needed rate. As the metabolic heat accumulates, it heats up the body. If that heating were to continue unabated, it would lead to death by hyperthermia at a core temperature of ∼315 K. As we will now discuss, however, this argument relies on assumptions that can be described as either overly pessimistic (tending to lower the predicted fatal T_w) or overly optimistic (tending to raise the predicted fatal T_w), raising the question of how accurate 308 K is as a threshold for survivability.

The *pessimistic* assumption is that a skin temperature higher than 308 K would be fatal. In reality, the human body is capable of moving basal metabolic heat from the core to the skin with a range of core-skin temperature differences. The body accomplishes this by changing the effective thermal conductivity between the core and skin by modulating the rate of core-to-skin blood flow. When the human starts to experience heat stress, skin blood flow increases, increasing the thermal conductance between the core and the skin, which makes the skin temperature approach the core temperature of 310 K (Stolwijk and Hardy 1966). So, only at a skin temperature close to 310 K is the core temperature guaranteed to rise. And even if the skin temperature is raised above 310 K, this does not necessarily imply heat death: it simply means the core temperature will also equilibrate to a similar temperature (Stolwijk and Hardy 1966, Gagge *et al* 1972, Rowell 1974). Fit individuals can survive a core temperature that is elevated by a few degrees. It is when the core temperature reaches about 315 K that the hyperthermia becomes fatal (e.g. Ferris *et al* 1938, Bouchama and Knochel 2002, SH10). Thus, only a skin temperature near or above 315 K is necessarily fatal.

On the other hand, SH10 made some assumptions that could be described as overly *optimistic*. The first was the omission of radiative exchange between the skin and the surroundings. SH10 justified this by assuming what they called 'gale-force winds,' guaranteeing that the exchange of energy between the skin and its surroundings is dominated by turbulent fluxes. But, using ERA5 reanalysis (Hersbach *et al* 2020) and a map of world population (CIESIN 2018), we find that an average of 98% of people are in locations where the windspeed is less than 4 m s^{-1} at any moment in time. This suggests that the exchange of infrared radiation is an important consideration. Since the radiating temperature only needs to exceed the skin temperature of ∼308 K to be a net source of radiative power to the body, the assumption of gale-force winds is overly optimistic in very hot conditions. Indeed, a recent experiment (Vecellio *et al* 2022) demonstrates that when exercising in a chamber with a low wind speed, even young, healthy adults start to have elevated core temperatures at a wet-bulb temperature well below 308 K. Furthermore, SH10 assumed that the humans who are outdoors have a resting metabolic rate around 50 W m^{-2}. This is an overly optimistic assumption for most outdoor workers.

Given this mix of overly pessimistic and optimistic assumptions, it is not clear *a priori* whether a wet-bulb threshold of 308 K is an overestimate or underestimate of what is truly survivable. To properly account for a finite wind speed, metabolic heat production, and radiative exchange, we must use a physiological model of thermoregulation, as provided by the model underlying the heat index (Steadman 1979a, Lu and Romps 2022).

2. The heat index

For a given temperature and humidity, the heat index is defined as the air temperature at a reference water-vapor pressure of 1.6 kPa that would be experienced in the same way by a healthy, acclimatized adult walking in the shade. The equivalence of experience is defined via the heat index's model of human thermoregulation, which uses a combination of physiological and behavioral strategies to regulate the core temperature at the standard value of 310 K (37 °C, 98.6 °F). In particular, two pairs of temperature and humidity are equivalent from the human perspective if the human naturally adopts the same behavior (e.g. same choice of clothing) and physiological state (e.g. same skin blood flow) in both.

Like the wet-bulb temperature, the heat index has been widely used to assess the risk of humid heat (Delworth *et al* 1999, Robinson 2001, Kim *et al* 2006, Diffenbaugh *et al* 2007, Yip *et al* 2008, Smith *et al* 2013, Wu *et al* 2014a, Oleson *et al* 2015, Opitz-Stapleton *et al* 2016, Diem *et al* 2017, Lyon and Barnston 2017, Modarres *et al* 2018, Tustin *et al* 2018, Xie *et al* 2018, Dahl *et al* 2019, Rao *et al* 2020, Rahman *et al* 2021, Amnuaylojaroen *et al* 2022, Perera *et al* 2022). Compared to the wet-bulb temperature, however, the heat index represents the next level of sophistication and realism when it comes to representing heat stress: it incorporates a realistic metabolic rate, infrared radiation, and the body's ability to alter its core-to-skin conductance. As the heat index increases, a person eventually runs out of options for regulating their core temperature at 310 K, resulting in hyperthermia. In such conditions, the heat index model predicts the new, higher temperature at which the core will equilibrate, enabling an assessment of survivability.

SH10 treated hyperthermia and heat death as closely related, but these two health outcomes occur at distinctly different values of the heat index: 345 K for hyperthermia and 366 K for heat death (Lu and Romps 2022).[4] When the heat index is less 345 K, the human is able to regulate the core temperature at 310 K, possibly with an elevated skin temperature. When the heat index exceeds 345 K, the skin temperature comes very close to the core temperature, and the core temperature is forced to rise. While undesirable, a fit and healthy adult can still survive with an elevated core temperature so long as it remains below the fatal value of 315 K. Only with sustained exposure to a heat index exceeding 366 K will the core temperature rise to 315 K (see Lu and Romps 2022, for the timescales involved).

Regarding Earth's future habitability, there are several uncertainties. For example, it is unknown what time series of greenhouse-gas emissions humankind will generate, with any given emissions scenario depending on multiple assumptions about socioeconomic and technological developments (e.g. Taylor *et al* 2012).[5] Even if the future emissions scenario were known, survivability can differ significantly across populations. For instance, elderly individuals (Deschênes and Moretti 2009, Carleton *et al* 2022) and those suffering from obesity (Dervis *et al* 2016) or cardiovascular disease (Gostimirovic *et al* 2020, Peters and Schneider 2020) are particularly susceptible to heat-related illnesses. Since people with different underlying health conditions and adaptive capacities will respond differently to the same climate (Vanos *et al* 2020), future habitability will depend, in part, on future demographics. In addition, the unknown amount of future acclimatization (Schickele 1947, Gubernot *et al* 2013, Arbury *et al* 2014, 2016, Folkerts *et al* 2020) and behavioral adaptation, such as the prevalence of air conditioning (O'Neill *et al* 2005), adds to the uncertainty.

To make progress in spite of these complexities, we take the following approach. First, to sidestep the uncertainty in future emissions, we study potential health outcomes not as a function of time, but as a function of global mean temperature. For example, in the RCP8.5 scenario, many climate models predict an increase in global mean temperature of about +4 K in 2100 relative to the pre-industrial period. Of course, some other models and scenarios reach +4 K earlier, some reach +4 K later, and some reach +4 K never. Rather than focusing on *when*, we focus on *how hot* and study, e.g. the potential health outcomes of a +4 K world, assuming that regional warming (and extreme heat in particular) is, to good approximation, a function of the global mean temperature (e.g. Seneviratne *et al* 2016, Wartenburger *et al* 2017).

Second, regarding demographics, we use the heat-index model, which is specifically designed to model the thermoregulation of fully acclimatized, young, healthy adults. The heat-index model assumes that these young, healthy adults can sweat profusely, can maintain large core-to-skin blood flow, and have an optimal (i.e. unabashed) approach to clothing. Therefore, by construction, this approach gives an upper limit on anyone's ability to avoid hyperthermia and heat death. Despite its idealizations, the heat-index model has recently been validated against empirical data gathered from young and healthy adults in a laboratory (Lu and Romps 2023): in the experiment, young and healthy adults were put in a climate chamber, and the temperature or humidity was slowly increased until the subjects started to experience hyperthermia (Wolf *et al* 2022). Lu and Romps (2023) showed that the heat index of 345 K (71.5 °C) accurately predicts the onset of hyperthermia in those experiments. Given this validated model for the young and healthy, we do not attempt to model future demographics or the impacts of high heat and humidity on the elderly, those with underlying medical conditions, or those who are poorly acclimatized. It must be borne in mind that those groups will tend to suffer serious health impacts at lower heat-index thresholds than are used in this study.

Third, we avoid the issue of air conditioning and its uncertain availability in future decades by focusing on the habitability of the outdoors. The pre-industrial Earth was supremely habitable in the sense that a person with appropriate clothing, water, and shade could survive the combination of temperature and humidity found anywhere on the planet. This made the outdoors almost universally accessible for work, pleasure, and exploration. In the future, this cannot be taken for granted. Here, we apply the heat-index model to outdoor temperature and humidity, which provides a physiological assessment of an acclimatized, young, healthy person outdoors in the shade.

3. Climate model results

As mentioned in the previous sections, a single value of the wet-bulb temperature ($T_w = 308$ K) is often used as a threshold of survivability, while the heat index has two thresholds: one for hyperthermia (HI = 345 K) and the other for heat death (HI = 366 K). We can quantify the frequencies of these thresholds by looking at a reanalysis and a global climate model. The left panel of figure 1 shows the historical (from 1996 to 2005, inclusive) global population-weighted distributions of instantaneous temperature T (black), annual maximum temperature T_{max} (blue), annual maximum

[4] More precise values are 344.65 and 366.44 K, respectively.

[5] Land use change can also add complexity to it due to, e.g. urban heat island or irrigation effects (Mishra *et al* 2020, Guo *et al* 2022).

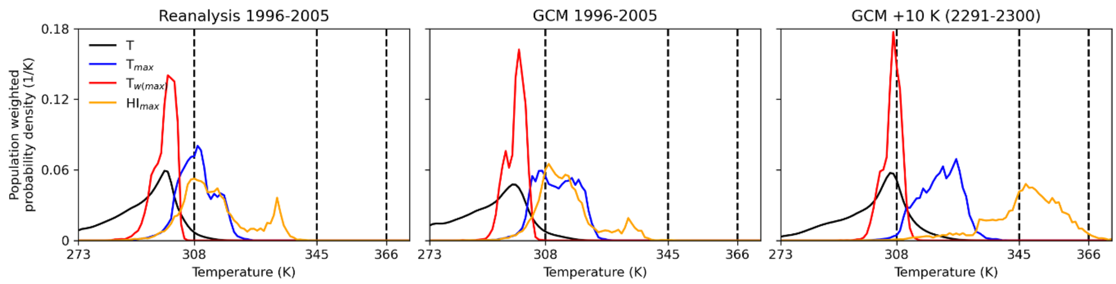

Figure 1. (left panel) The global population-weighted distribution of hourly temperature (black), yearly maximum temperature (blue), yearly maximum wet-bulb temperature (red) and the yearly maximum heat index (orange) calculated using ERA5 reanalysis data over the entire globe during 1996–2005, inclusive. (middle panel) Same, but calculated using CNRM-CM5 3-hourly historical data during 1996–2005. (right panel) Same, but calculated using CNRM-CM5 simulation of the RCP8.5 scenario 3-hourly data during 2291–2300, which has a global mean temperature anomaly of +10 K relative to preindustrial. The dashed vertical lines mark $T_w = 308$ K (SH10 proposal), HI = 345 K (hyperthermia), and HI = 366 K (heat death given sustained exposure).

wet-bulb temperature $T_{w(max)}$ (red), and annual maximum heat index HI_{max} (orange) from ERA5 hourly reanalysis (Hersbach *et al* 2020) and a map of world population in 2005 (CIESIN 2018). Although using ERA5 1996–2005 instead of ERA-Interim 1999–2008 as in SH10, the curves shown here qualitatively match the curves shown in figure 1A of SH10, which also used a 60S-to-60N land area weighting instead of the population weighting used here. The middle panel shows the same curves calculated from the historical (1996–2005)[6] simulations of the CNRM-CM5 climate model (Voldoire *et al* 2013) from the CMIP5 archive (Taylor *et al* 2012).[7] Its curves closely match the curves calculated from the reanalysis, bolstering confidence in the climate-model output. The right panel shows the curves calculated from the CNRM-CM5 simulation of the RCP8.5 scenario in the decade 2291–2300, during which the global mean temperature was 9.2 K higher than in the 1996–2005 historical period and 10 K higher than the 1850–1900 preindustrial period (henceforth referred to as the '+10 K world'). Following SH10, we use this worst-case scenario to illustrate what would happen in extreme warming. As in figure 1C of SH10, the distribution of $T_{w(max)}$ in this period of extreme warmth straddles 308 K (35 °C), marked by a dashed line.

As in SH10, the ERA5 reanalysis shows that the historical climate has no wet-bulb temperatures higher than 308 K and no heat index higher than 345 K. On the other hand, 26% of the world's current population lives in locations that would, in a typical year, expose them to $T_w > 308$ K in a +10 K world. We find, however, that only a small fraction of those locations would be fatal for a young and healthy person. Using the heat index, we find that only 1.7% of the current population lives in places in which sustained walking in outdoors shade would be lethal ($HI > 366$ K) on some day of the year in a +10 K world. But we find that a majority (62%) of people currently live in places that will be intolerable in the sense that, at some point during the year, a young, healthy adult walking in the shade would not be able to maintain a normal core temperature ($HI > 345$ K).

To reveal the spatial and temporal distributions of these exceedances ($T_w > 308$ K, $HI > 345$ K, $HI > 366$ K), we plot the map of the return period of each exceedance in figure 2 for the +10 K world. The shortest return period for each exceedance is shown at the bottom right of the map. SH10 used a climate simulation with a slightly higher global-mean temperature than shown here, but the locations of finite return time in the left panel of figure 2 are approximately the same locations with $T_{w(max)} > 308$ K in figure 1F of SH10: large swath of Africa, Australia, Arabia, India, South America, Eastern China, and the Midwestern and Eastern United States. But the maps of recurrence time of $HI > 345$ K and $HI > 366$ K, shown in the middle and right panels of figure 2, respectively, are qualitatively different. The places predicted to be consistently (once or more per year) fatal ($HI > 366$ K) to a young, healthy person taking a sustained walk in the shade are the Amazon rainforest, the Sahara desert, the Congo Basin, and the Arabian Peninsula. Other locations that become marginally lethal include parts of eastern China from Shanghai to Beijing and parts of the Midwest United States. The hyperthermic locations ($HI > 345$ K), however, are much more widespread than predicted by the wet-bulb threshold. Those regions of hyperthermia cover the entire middle and lower latitudes, with a shortest return period of 2 days. In the United States, for example, the Midwest and East Coast see a heat index of 345 K with recurrence times ranging from a few years to a few months. Notably, some of the *shortest* return periods for hyperthermia occur among the *most densely* populated regions of the world,

[6] The period of 1996–2005 is chosen as the baseline because it covers the last ten years in the CMIP5 historical simulations.
[7] CNRM-CM5, bcc-csm1-1, and IPSL-CM5A-LR are the only three CMIP5 climate models for which we could obtain 3-hourly data in the extended RCP8.5 scenarios. We use CNRM-CM5 to make figures 1 and 2 because it has the highest spatial resolution. Later, in figure 3 and in the sensitivity-test section, we will use all of the three models and compare their results.

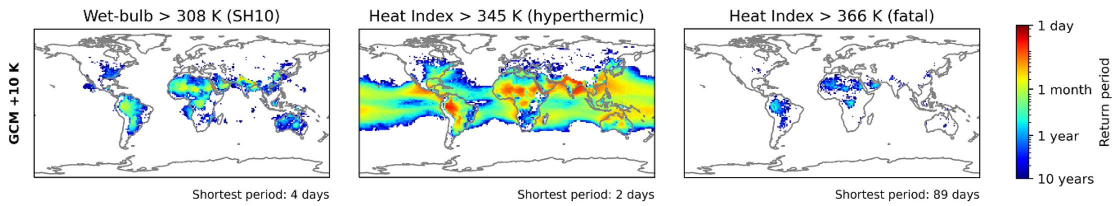

Figure 2. The return period for (left) wet-bulb temperature exceeding the widely used threshold value of 308 K, (middle) the heat index exceeding the hyperthermic value of 345 K, and (right) the heat index exceeding the fatal value of 366 K, as calculated from CNRM-CM5 RCP8.5 data during 2291–2300, which has a global mean temperature anomaly of +10 K relative to the preindustrial mean. The subscript at the right bottom of each map shows the shortest return period in that particular map during 2291–2300.

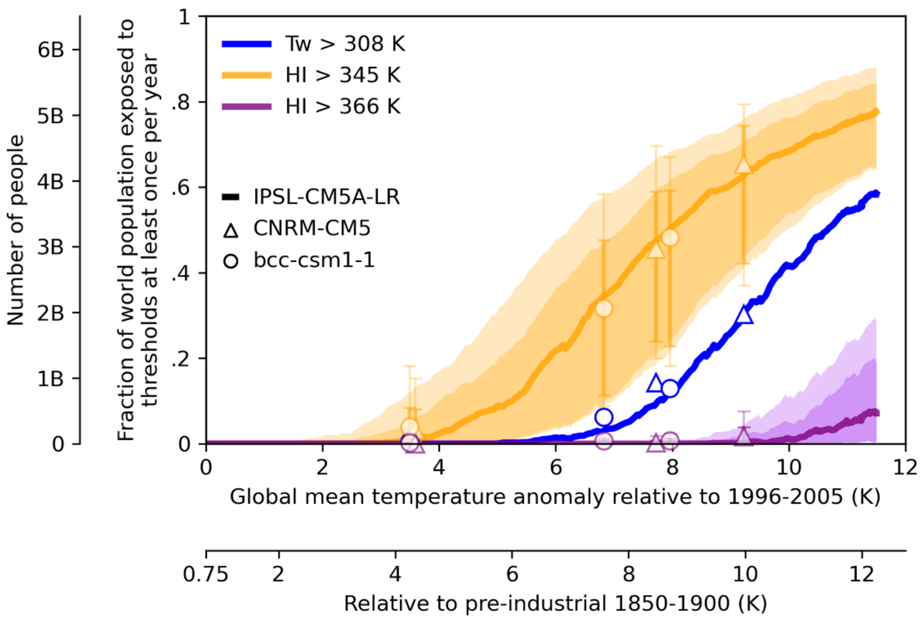

Figure 3. The fraction of the 2005 world population experiencing three criteria: wet-bulb temperatures greater than 308 K (blue), heat index greater than 345 K (hyperthermic; orange), and heat index greater than 366 K (fatal; purple) as functions of the global-mean temperature anomaly relative to 1996–2005. The curves plot these fractions for the IPSL-CM5A-LR simulation of RCP8.5 scenario from 2006–2300, inclusive. A ten-year-window averaging is applied to each year smooth the curves. The symbols have the same meaning as the curves, but are calculated using the CNRM-CM5 (round) and the bcc-csm1-1 (triangle) simulations, averaged over the last ten years of the 21st, 22nd and 23rd centuries. The light shadings and the thin error bars are the spreads due to a range of metabolic rates of 50–300 W m^{-2}, and the dark shadings and thick error bars are the spreads due to a range of windspeed of 1–4 m s^{-1}. The floating ordinate shows the corresponding world population in 2005, and the floating abscissa shows the global mean temperature anomaly relative to the pre-industrial period of 1850–1900.

e.g. Bangladesh and northern India. That results in a significant proportion of the world's population experiencing hyperthermia.

To illustrate how much of the current (2005) world population would be exposed to critical thresholds at different global-mean temperature anomalies, we use the RCP8.5 scenario in the IPSL-CM5A-LR climate model (Dufresne *et al* 2013), which has a coarser resolution than CNRM-CM5 but has a 3-hourly output for the entire period of 2006–2300. The IPSL-CM5A-LR model also has a higher global mean temperature anomaly of +12.3 K (relative to preindustrial) during 2291–2300, compared to +10 K for CNRM-CM5, allowing a wider temperature range to be probed. The blue curve in figure 3 shows the fraction of world population exposed to $T_w > 308$ K at least once a year in IPSL-CM5A-LR. Similarly, the orange and purple curves are the fractions of world population exposed to a heat index higher than 345 K and 366 K, respectively, at least once per year. These sandwich the blue curve, delivering the same message that the 308 K wet-bulb temperature threshold underestimates the frequency of hyperthermia, but overestimates the frequency of heat death. To smooth the curves, a ten-year averaging window has been applied.

On top of each curve, we plot the results from two other global climate models, CNRM-CM5 and bcc-csm1-1 (Wu *et al* 2014b), as round and triangle symbols, respectively. Each symbol represents a ten-year average of the annual fraction of world population exposed to the given threshold during the last ten years of the 21st, 22nd and 23rd centuries. Due to their finer resolution, CNRM-CM5 and bcc-csm1-1 do not output 3-hourly data over the entire extended RCP8.5 period of 2006–2300, and, therefore, we show the time intervals during which data are available. Each symbol is horizontally located at its ten-year mean temperature anomaly. Notice that the three global climate models have different temperature anomalies at the end of each century in the extended RCP8.5 scenarios: for example, in 2291–2300, the temperature anomalies are +12.3 K in IPSL-CM5A-LR, +10 K in CNRM-CM5, and +8.7 K in bcc-csm1-1. Although these models forecast different temperatures for a given time interval, they predict very similar population exposures at a given amount of warming.

Added to figure 3 is a floating ordinate showing the corresponding world population in 2005. Roughly speaking, in a world warmer than pre-industrial by 10 K, around 30% of the world's population (about 2 billion people) would be exposed once or more per year to a wet-bulb temperature above 308 K, while less than 2% (about 100 million people) would be exposed to fatal conditions and over 60% (nearly 4 billion people) would be exposed to conditions that would cause hyperthermia.

4. Sensitivity test

The heat index assumes a metabolic rate at 180 W m^{-2} and an overall wind speed of 1.5 m s^{-1}. This metabolic rate corresponds to a walking pace at 1.4 m s^{-1} (Steadman 1979b, Parsons 2014), and that overall wind speed is converted from the heat transfer coefficient of 12.3 W m^{-2} K^{-1} in Steadman's model (Steadman 1979a) using Churchill and Bernstein's relation (Churchill and Bernstein 1977). Here, we will calculate how sensitive the hyperthermic and fatal thresholds are to these assumptions.

Using the ERA5 wind speed and the roughness length data, and assuming a log-profile wind structure, we find that, at any moment in time, 98% of the population experiences wind speeds less than 4 m s^{-1} at half of the assumed human height of 0.85 m (Steadman 1979a). To explore a range of plausible wind speeds, we will therefore vary the wind speed u in the heat index model from 1 to 4 m s^{-1}, where the lower bound of 1 m s^{-1} is chosen to represent the wind induced by human motion and natural convection. Similarly, to explore different levels of physical exertion, we will use previously defined exertion levels (Ainsworth *et al* 1993), which define a metabolic rate of 50–150 W m^{-2} as light activity and 150–300 W m^{-2} as moderate activity. Any activity requiring a metabolic rate beyond 300 W m^{-2} is considered vigorous. We assume a person would have the freedom and commonsense to avoid vigorous activity during heat stress, and thus we vary the metabolic rate Q over 50–300 W m^{-2}. Note that a resting metabolic rate of 50 W m^{-2} is included in our sensitivity test as the lower bound.

To perform this sensitivity analysis, we must generalize the heat index to an apparent temperature that takes two extra arguments (u and Q) besides the air temperature and humidity. The procedure is a straightforward modification of the heat index. In particular, the apparent temperature for a given T_a, p_v, u, and Q is the air temperature at a $p_{v0} = 1.6$ kPa, $u_0 = 1.5$ m s^{-1}, and $Q_0 = 180$ W m^{-2} that would feel the same in the sense of generating the same behavior (choice of clothing) and same physiology (skin blood flow, equilibrium core temperature). Because the reference state (p_{v0}, u_0, Q_0) is the same as in the original heat index, the apparent temperature generated in this way has the same interpretation, e.g. an apparent temperature of 345 K (366 K) is still the threshold for hyperthermia (lethality).

The results of the sensitivity analysis are shown in figure 3 as the shadings around the curves and the error bars on the symbols. The dark shading and bars show the spread due to varying u from 1 to 4 m s^{-1} and the light shading and bars show the spread due to varying Q over 50–300 W m^{-2}. The wet-bulb temperature depends on neither u nor Q, so adjusting those parameters has no effect on the blue curve. We see that the plausible changes to the metabolic rate or the wind speed effectively shift the orange and purple curves left or right on the abscissa by ∼1–2 K. For example, 10% of the world's population would experience hyperthermic conditions walking in the shade with about 5 K of additional warming (relative to 1996–2005), but 10% of the population would experience hyperthermia performing 300 W m^{-2} of moderate work in the shade with only 3 K of additional warming. Notably, even with these variations in assumed parameters, the commonly used T_w threshold (blue curve) still overestimates lethality and underestimates hyperthermia.

5. Discussion

We have shown that the commonly used wet-bulb-temperature threshold of 308 K (35 °C) underestimates the prevalence of hyperthermia and overestimates the prevalence of fatalities. Implicit in the derivation of $T_w = 308$ K as a critical threshold is the assumption that a person is exposed to a wind speed equal to a strong breeze or greater, which would enhance the body's evaporative cooling. In reality, people are usually exposed to much more stagnant winds and, in hot conditions, they absorb infrared radiation from surrounding surfaces that are hotter than their core temperature. This leads to an onset of hyperthermia at wet-bulb temperatures less than 308 K. On the other hand, using $T_w = 308$ K as a fatal threshold is too pessimistic because an elevated core temperature is not necessarily fatal. Only when the core temperature equilibrates at or above 315 K is heat death a common outcome, and this occurs at wet-bulb temperatures greater than 308 K. It is worth noting, however, that this hinges on the assumption of a typical outdoor wind speed in the range of 1–4 m s^{-1}. For a person exerting themselves indoors, where the wind speed is measured in tens of centimeters per second, fatal conditions are typically reached at wet-bulb temperatures lower than 308 K (Lu and Romps 2023).

The three climate models studied here are in broad agreement about the amount of warming that leads to severe health outcomes for people outdoors in the shade. Hyperthermia would start to be a regular occurrence at a global-mean warming of about +3 K relative to preindustrial. For a higher warming of +4 K relative to preindustrial, a large number of people, measured in tens of millions or hundreds of millions, would be exposed to hyperthermic conditions at least once per year. On the other hand, a global-mean temperature anomaly of around +10 K is needed to generate fatal conditions for ~100 million people every year. As mentioned in section 2, it is important to note that these global-mean temperature thresholds for hyperthermia and fatality would be lower if considering people who are in the sun, or people who are exerting themselves to a greater degree, or people with underlying health conditions or age-related declines in sweating capacity or cardiovascular fitness.

Data availability statement

The data that support the findings of this study are openly available at the following URL/DOI: https://esgf-node.llnl.gov/search/cmip5/.

Acknowledgments

The authors are grateful to William R Boos and the reviewers for helpful feedback. Code for calculating the heat index is available in R, Python, and Fortran at https://romps.berkeley.edu/papers/pubs-2020-heatindex.html.

ORCID iDs

Yi-Chuan Lu https://orcid.org/0000-0003-3659-1474
David M Romps https://orcid.org/0000-0001-7649-5175

References

Ainsworth B E, Haskell W L, Leon A S, Jacobs D R, Montoye H J, Sallis J F and Paffenbarger R S 1993 Compendium of physical activities: classification of energy costs of human physical activities *Med. Sci. Sports Exerc.* **25** 71–80

Amnuaylojaroen T, Limsakul A, Kirtsaeng S, Parasin N and Surapipith V 2022 Effect of the near-future climate change under RCP8.5 on the heat stress and associated work performance in Thailand *Atmosphere* **13** 325

Arbury S, Jacklitsch B, Farquah O, Hodgson M, Lamson G, Martin H and Profitt A 2014 Heat illness and death among workers—United States, 2012–2013 *Morb. Mortal. Wkly. Rep.* **63** 661

Arbury S, Lindsley M and Hodgson M 2016 A critical review of OSHA heat enforcement cases *J. Occup. Environ. Med.* **58** 359–63

Bouchama A and Knochel J P 2002 Heat stroke *New Engl. J. Med.* **346** 1978–88

Carleton T *et al* 2022 Valuing the global mortality consequences of climate change accounting for adaptation costs and benefits *Q. J. Econ.* **137** 2037–105

Churchill S W and Bernstein M 1977 A correlating equation for forced convection from gases and liquids to a circular cylinder in crossflow *J. Heat Transfer* **99** 300–6

CIESIN 2018 *Gridded Population of the World, Version 4 (GPWv4): Population Count, Revision 11* (NASA Socioeconomic Data and Applications Center (SEDAC)) (https://doi.org/10.7927/H4JW8BX5)

Coffel E D, Horton R M and de Sherbinin A 2017 Temperature and humidity based projections of a rapid rise in global heat stress exposure during the 21st century *Environ. Res. Lett.* **13** 014001

Dahl K, Licker R, Abatzoglou J T and Declet-Barreto J 2019 Increased frequency of and population exposure to extreme heat index days in the United States during the 21st century *Environ. Res. Commun.* **1** 075002

Delworth T L, Mahlman J D and Knutson T R 1999 Changes in heat index associated with CO_2-induced global warming *Clim. Change* **43** 369–86

Dervis S, Coombs G B, Chaseling G K, Filingeri D, Smoljanic J and Jay O 2016 A comparison of thermoregulatory responses to exercise between mass-matched groups with large differences in body fat *J. Appl. Physiol.* **120** 615–23

Deschênes O and Moretti E 2009 Extreme weather events, mortality and migration *Rev. Econ. Stat.* **91** 659–81

Diem J E, Stauber C E, Rothenberg R and Añel J A 2017 Heat in the southeastern United States: characteristics, trends and potential health impact *PLoS One* **12** e0177937

Diffenbaugh N S, Pal J S, Giorgi F and Gao X 2007 Heat stress intensification in the Mediterranean climate change hotspot *Geophys. Res. Lett.* **34** L11706

Dufresne J-L *et al* 2013 Climate change projections using the IPSL-CM5 earth system model: from CMIP3 to CMIP5 *Clim. Dyn.* **40** 2123–65

Ferris E B, Blankenhorn M A, Robinson H W and Cullen G E 1938 Heat stroke: clinical and chemical observations on 44 cases *J. Clin. Invest.* **17** 249–62

Folkerts M A, Bröde P, Botzen W J W, Martinius M L, Gerrett N, Harmsen C N and Daanen H A M 2020 Long term adaptation to heat stress: shifts in the minimum mortality temperature in the Netherlands *Front. Physiol.* **11** 225

Gagge A P, Stolwijk J A J and Nishi Y 1972 An effective temperature scale based on a simple model of human physiological regulatory response *ASHRAE Trans.* **77** 247–62

Gostimirovic M, Novakovic R, Rajkovic J, Djokic V, Terzic D, Putnik S and Gojkovic-Bukarica L 2020 The influence of climate change on human cardiovascular function *Arch. Environ. Occup. Health* **75** 406–14

Gubernot D M, Anderson G B and Hunting K L 2013 The epidemiology of occupational heat exposure in the United States: a review of the literature and assessment of research needs in a changing climate *Int. J. Biometeorol.* **58** 1779–88

Guo Q, Zhou X, Satoh Y and Oki T 2022 Irrigated cropland expansion exacerbates the urban moist heat stress in northern India *Environ. Res. Lett.* **17** 054013

Hersbach H *et al* 2020 The ERA5 global reanalysis *Q. J. R. Meteorol. Soc.* **146** 1999–2049

Im E-S, Kang S and Eltahir E A B 2018 Projections of rising heat stress over the western Maritime Continent from dynamically downscaled climate simulations *Glob. Planet. Change* **165** 160–72

Im E-S, Pal J S and Eltahir E A B 2017 Deadly heat waves projected in the densely populated agricultural regions of South Asia *Sci. Adv.* **3** e1603322

Kim H, Ha J-S and Park J 2006 High temperature, heat index and mortality in 6 major cities in South Korea *Arch. Environ. Occup. Health* **61** 265–70

Lu Y-C and Romps D M 2022 Extending the heat index *J. Appl. Meteorol. Climatol.* **61** 1367–83
Lu Y-C and Romps D M 2023 Predicting fatal heat and humidity using the heat index model *J. Appl. Physiol.* **134** 649–56
Lyon B and Barnston A G 2017 Diverse characteristics of US summer heat waves *J. Clim.* **30** 7827–45
Mishra V, Ambika A K, Asoka A, Aadhar S, Buzan J, Kumar R and Huber M 2020 Moist heat stress extremes in India enhanced by irrigation *Nat. Geosci.* **13** 722–8
Modarres R, Ghadami M, Naderi S and Naderi M 2018 Future heat stress arising from climate change on Iran's population health *Int. J. Biometeorol.* **62** 1275–81
Monteiro J M and Caballero R 2019 Characterization of extreme wet-bulb temperature events in southern Pakistan *Geophys. Res. Lett.* **46** 10659–68
O'Neill M S, Zanobetti A and Schwartz J 2005 Disparities by race in heat-related mortality in four US cities: the role of air conditioning prevalence *J. Urban Health* **82** 191–7
Oleson K W, Monaghan A, Wilhelmi O, Barlage M, Brunsell N, Feddema J, Hu L and Steinhoff D F 2015 Interactions between urbanization, heat stress and climate change *Clim. Change* **129** 525–41
Opitz-Stapleton S, Sabbag L, Hawley K, Tran P, Hoang L and Nguyen P H 2016 Heat index trends and climate change implications for occupational heat exposure in Da Nang, Vietnam *Clim. Serv.* **2–3** 41–51
Pal J S and Eltahir E A B 2016 Future temperature in southwest Asia projected to exceed a threshold for human adaptability *Nat. Clim. Change* **6** 197
Parsons K 2014 *Human Thermal Environments: The Effects of Hot, Moderate and Cold Environments on Human Health, Comfort and Performance* 3rd edn (Taylor & Francis) (https://doi.org/10.1201/b16750)
Perera T A N T, Nayanajith T M D, Jayasinghe G Y and Premasiri H D S 2022 Identification of thermal hotspots through heat index determination and urban heat island mitigation using ENVImet numerical micro climate model *Model. Earth Syst. Environ.* **8** 209–26
Peters A and Schneider A 2020 Cardiovascular risks of climate change *Nat. Rev. Cardiol.* **18** 1–2
Rahman M B, Salam R, Islam A, Tasnuva A, Haque U, Shahid S, Hu Z and Mallick J 2021 Appraising the historical and projected spatiotemporal changes in the heat index in Bangladesh *Theor. Appl. Climatol.* **146** 125–38
Ramsay E E, Fleming G M, Faber P A, Barker S F, Sweeney R, Taruc R R, Chown S L and Duffy G A 2021 Chronic heat stress in tropical urban informal settlements *iScience* **24** 103248
Rao K K, Kumar T V L, Kulkarni A, Ho C H, Mahendranath B, Desamsetti S, Patwardhan S, Dandi A R, Barbosa H and Sabade S 2020 Projections of heat stress and associated work performance over India in response to global warming *Sci. Rep.* **10** 16675
Raymond C, Matthews T and Horton R M 2020 The emergence of heat and humidity too severe for human tolerance *Sci. Adv.* **6** eaaw1838
Robinson P J 2001 On the definition of a heat wave *J. Appl. Meteorol. Climatol.* **40** 762–75
Rogers C D W, Ting M, Li C, Kornhuber K, Coffel E D, Horton R M, Raymond C and Singh D 2021 Recent increases in exposure to extreme humid-heat events disproportionately affect populated regions *Geophys. Res. Lett.* **48** e2021GL094183
Rowell L B 1974 Human cardiovascular adjustments to exercise and thermal stress *Physiol. Rev.* **54** 75–159
Saeed F, Schleussner C-F and Ashfaq M 2021 Deadly heat stress to become commonplace across South Asia already at 1.5 °C of global warming *Geophys. Res. Lett.* **48** e2020GL091191
Schär C 2016 Climate extremes: the worst heat waves to come *Nat. Clim. Change* **6** 128–9
Schickele E 1947 Environment and fatal heat stroke *Mil. Med.* **100** 235–56
Seneviratne S I, Donat M G, Pitman A J, Knutti R and Wilby R L 2016 Allowable CO_2 emissions based on regional and impact-related climate targets *Nature* **529** 477–83
Sherwood S C 2018 How important is humidity in heat stress? *J. Geophys. Res.: Atmos.* **123** 11808–10
Sherwood S C and Huber M 2010 An adaptability limit to climate change due to heat stress *Proc. Natl Acad. Sci.* **107** 9552–5
Smith T T, Zaitchik B F and Gohlke J M 2013 Heat waves in the United States: definitions, patterns and trends *Clim. Change* **118** 811–25
Steadman R G 1979a The assessment of sultriness. Part I: a temperature-humidity index based on human physiology and clothing science *J. Appl. Meteorol.* **18** 861–73
Steadman R G 1979b The assessment of sultriness. Part II: effects of wind, extra radiation and barometric pressure on apparent temperature *J. Appl. Meteorol.* **18** 874–85
Stolwijk J A and Hardy J D 1966 Partitional calorimetric studies of responses of man to thermal transients *J. Appl. Physiol.* **21** 967–77
Taylor K E, Stouffer R J and Meehl G A 2012 An overview of CMIP5 and the experiment design *Bull. Am. Meteorol. Soc.* **93** 485–98
Tustin A W, Lamson G E, Jacklitsch B L, Thomas R J, Arbury S B, Cannon D L, Gonzales R G and Hodgson M J 2018 Evaluation of occupational exposure limits for heat stress in outdoor workers—United States, 2011–2016 *Morb. Mortal. Wkly. Rep.* **67** 733
Vanos J K, Baldwin J W, Jay O and Ebi K L 2020 Simplicity lacks robustness when projecting heat-health outcomes in a changing climate *Nat. Commun.* **11** 6079
Vecellio D J, Wolf S T, Cottle R M and Kenney W L 2022 Evaluating the 35C wet-bulb temperature adaptability threshold for young, healthy subjects (PSU HEAT Project) *J. Appl. Physiol.* **132** 340–5
Voldoire A *et al* 2013 The CNRM-CM5.1 global climate model: description and basic evaluation *Clim. Dyn.* **40** 2091–121
Wartenburger R, Hirschi M, Donat M G, Greve P, Pitman A J and Seneviratne S I 2017 Changes in regional climate extremes as a function of global mean temperature: an interactive plotting framework *Geosci. Model Dev.* **10** 3609–34
Wolf S T, Cottle R M, Vecellio D J and Kenney W L 2022 Critical environmental limits for young, healthy adults (PSU HEAT Project) *J. Appl. Physiol.* **132** 327–33
Wu J, Zhou Y, Gao Y, Fu J S, Johnson B A, Huang C, Kim Y-M and Liu Y 2014a Estimation and uncertainty analysis of impacts of future heat waves on mortality in the Eastern United States *Environ. Health Perspect.* **122** 10–16
Wu T *et al* 2014b An overview of BCC climate system model development and application for climate change studies *J. Meteorol. Res.* **28** 34–56
Xie J, Chen Y, Hong T and Laing T D 2018 Relative humidity for load forecasting models *IEEE Trans. Smart Grid* **9** 191–8
Yip F Y, Flanders W D, Wolkin A, Engelthaler D, Humble W, Neri A, Lewis L, Backer L and Rubin C 2008 The impact of excess heat events in Maricopa County, Arizona: 2000–2005 *Int. J. Biometeorol.* **52** 765–72